ELSEVIER

Polymer 42 (2001) 6833–6839

polymer

www.elsevier.nl/locate/polymer

Effect of the size of the dispersed NBR phase in PVC/NBR blends on the stability of PVC to electron irradiation

Jian-Xiong Li, Chi-Ming Chan*

Department of Chemical Engineering, The Hong Kong University of Science and Technology, Advanced Engineering Materials Fac, Clear Water Bay, Kowloon, Hong Kong

Received 14 August 2000; received in revised form 12 December 2000; accepted 27 February 2001

Abstract

Acrylonitrile–butadiene copolymers (NBR) with different acrylonitrile contents were melt-mixed with poly(vinyl chloride) (PVC). The morphology of the blends was examined with transmission electron microscopy (TEM). The samples were also exposed to an electron beam and the chlorine-loss upon electron irradiation was monitored with electron dispersion X-ray analyzer (EDX). TEM results indicated that all samples blended with different NBR, including NBR-33 and NBR-41, were heterogeneous, but the dispersion of NBR-33 was the finest. The results of the chlorine-loss study showed that the radiation sensitivity of PVC was improved by the addition of NBR and the extent of improvement was strongly related to the miscibility. Analysis of experimental data demonstrated that chlorine loss of PVC/NBR blends followed the Vesely's double exponential equation but the coefficient and rate constants varied with different NBR. For polymer blends containing a component that is radiation insensitive and another component that is unstable under irradiation, such as a fluoropolymer and chloropolymer, the loss of fluorine or chlorine as a function of radiation dose can be used to compare the size of the dispersed phase of the polymer blends.

Keywords: PVC/NBR blends; Radiation resistance; Size of the NBR dispersed phase

1. Introduction

When a polymer is exposed to high-energy radiation, such as X-ray, γ-ray and high-energy electron beam, its composition and structure inevitably undergo some changes [1–4], which in turn lead to changes in physical and chemical properties of the polymers. The changes caused by high-energy radiation are complicated and so far have not been fully understood. A great deal of effort has been devoted to studies in this area and some advances have been made, especially in the mechanisms at the initial stage of irradiation [1–2]. At the initial stage, the high-energy radiation is much less selective to the nature of the primary bonds of a polymer owing to the extreme high energy of the radiation compared to the dissociation energy of the primary bonds. When a high-energy photon or electron is sufficiently close to an organic molecule, it will cause local polarization (even ionization) of the atoms and, therefore, create a highly excited state. The excitation energy can be dissipated in a number of ways — the excited molecules may decompose into free radicals or ion radicals and then initiate various chemical reactions. The exact reaction process, reaction rate, and resultant products are different for different polymers. They depend on the molecular structure, chemical environment, and exposure dose. Nevertheless, it is believed that free radical reaction is predominant in polymers, and as a result of irradiation, the chain scission, cross-linking, and formation of volatile products may occur simultaneously in a similar fashion as the free radical chain reaction.

There are two common ways to protect an organic polymer from degradation by the high energy radiation — the excitation energy is transferred to another medium before chemical reactions are initiated or the radicals are trapped in these chemical reactions [1–3]. Aromatic groups are known to be radiation-stable because they can dissipate the excitation energy as heat in various vibration modes [2] and trap radicals. The incorporation of phenyl rings into the polymer chains has been used to enhance the radiation stability of some radiation-sensitive polymers. The replacement of the methyl group of polydimethylsiloxane by a phenyl group [5], the copolymerization of isobutene with styrene [2], and the attachment of phenyl rings to the methacrylate backbone [6] are typical examples. However, the protection offered by a radiation-insensitive polymer to a radiation-sensitive polymer in a blend is still inconclusive. For example, the

* Corresponding author. Tel./fax: +852-2358-1725.
E-mail address: kecmchan@ust.hk (C.-M. Chan).

0032-3861/01/$ - see front matter
PII: S0032-3861(01)00179-3

blending of PMMA with PS only gave a marginal protective effect to PMMA [7] while blending with styrene-co-acrylonitrile copolymer (SAN) led to a significant decrease in the scission of PMMA upon γ-radiation in vacuum [8]. The difference in radiation sensitivity between these two blends was interpreted on the basis of the miscibility of the polymer pairs. It was believed that PMMA was immiscible with PS and blending PMMA and PS would generate a coarse phase structure owing to phase segregation; hence, the short range protective effect of phenyl groups in PS was minimized in the immiscible blends. Similar effects were found in the PVC blends [9].

Polyvinyl chloride (PVC) and other chlorinated polyolefins are known to be highly sensitive to high-energy radiation. In these chlorinated polymers, the carbon–chlorine bond is weaker than both the carbon–carbon bond and the carbon–hydrogen bond; therefore, upon exposure to high-energy radiation some of the carbon–chlorine bonds are broken, giving rise to organic radicals and chlorine radicals. The chlorine radicals will attract hydrogen atoms and initiate dehydrochlorination, liberating volatile hydrogen chlorine and resulting in a less radiation-sensitive polyene structure in the backbone. Vesely and Finch suggested that the radiation-induced dehydrochlorination in PVC was an autocatalytic reaction [10]. They believed that the rapid dehydrochlorination of PVC was attributed to the long regular sequences.

Several mathematical models have been put forward to describe the chlorine loss in PVC upon electron irradiation. Delgado and Hutchinson [11] investigated the dehydrochlorination of PVC with EDX and described the chlorine decay by a single-exponential function:

$$I = I_0\exp(-D/\tau) + I_\tau, \tag{1}$$

where I is the measured intensity of Cl K line at exposure D in C m^{-2} and I_0, τ and I_τ are constants. Isaacson [12] has also used a single-exponential function with an offset to fit the data from the literature, but he found the correlation between the equation and experimental data was poor. Egerton [13] suggested a double-exponential function to describe the chlorine-loss data:

$$I/I_0 = \exp(-C_1D) + \exp(-C_2D), \tag{2}$$

where I/I_0 is the normalized intensity from the elemental peak, C_1 and C_2 are constants. Vesely and Finch [10,14–15] pointed out that the radiation-induced dehydrochlorination of PVC consisted of two independent chemical processes — a fast and a slow one. The fast process mainly involved the long regular sequences in original PVC while the slower one became predominant for the disturbed structure at higher exposures. The chlorine decay could be best described in a double-exponential function in the following form:

$$I/I_0 = (1 - A)\exp(-k_1D) + A\exp(-k_2D), \tag{3}$$

where k_1 and k_2 are the decay constants for the fast and slow processes, respectively, and A is the concentration of the less radiation-sensitive portion. As an approximation at low radiation exposures, the double-exponential equation was simplified in the form:

$$I/I_0 = (1 - A)\exp(-k_1D) + A. \tag{4}$$

In our previous work [16], an unsaturated rubber (polystyrene-co-butadiene, SBR) was blended with PVC and the stability of PVC to electron irradiation was improved. The radiation stability of PVC in the PVC/SBR blend was further enhanced by the addition of an acrylonitrile-butadiene (NBR) rubber as a compatibilizer. The improvement of radiation stability was attributed to the transfer of active radicals to the unsaturated double bonds. NBR was believed to have improved the molecular contact between the PVC and SBR phases and to enhance the reaction probability between radicals and double bonds.

It is well known that the size of the dispersed NBR phase in NBR/PVC blends varies with the acrylonitrile content [17–19]. Therefore, the degree of molecular contact between PVC and NBR is expected to be different when PVC is blended with NBR with a different acrylonitrile content. Thus, it may be possible to use the decay of the chlorine signal as a function of radiation dose to compare the size of the dispersed NBR phase of the blends. Furthermore, since the radiation protection requires intimate contacts between the radiation sensitive and insensitive components, it may be possible to use the decay of fluorine or chlorine signal as a function of radiation dose to compare the size of the dispersed phase in some fluoropolymer or chloropolymer blends.

2. Experimental

2.1. Materials

The acrylonitrile-butadiene rubbers (NBRs) used in this work were purchased from Scientific Polymer Products, Inc. Four copolymers with different acrylonitrile contents were selected and their composition and viscosity are summarized in Table 1. The K value of polyvinyl chloride (PVC) is 67 (Fikenstcher DIN 53726). Other additives incorporated in the PVC/NBR blends were of commercial grades.

2.2. Preparation of PVC/NBR blends

The blending was performed using a Haake Rheometer 9000 equipped with a 600 mixer and two Banbury rotors. The PVC resin mixed with additives was first charged into

Table 1
Acrylonitrile content and viscosity of acrylonitrile-co-butadiene rubber

	NBR-21	NBR-33	NBR-41	NBR-51
Acrylonitrile content (%)	21	33	41	51
Mooney viscosity	60	55	60	55

the chamber of the mixer and processed for 4 min, NBR was then added. Five parts of stabilizers and processing aids were used. The wall temperature of the mixer was controlled at 150°C and the rotors were operated at 30 rpm. After blending for another 20 min, the compound was discharged and compression molded into 2 mm thick plates at 165°C for 10 min. Two series of PVC/NBR blends were prepared, one containing 10 parts of NBR and the other 25 parts.

2.3. TEM

The compression molded samples were cut into 80 nm thick sections on a Reichert–Jung Ultracut R microtome with a diamond knife. The preparation of the section was conducted at 1.0 mm s^{-1} at approximately −100°C. The ultrathin sections were mounted on 300-mesh copper grids and dried in a desiccator for 2 h before being put in the vapor of ruthenium tetroxide over a 0.3% aqueous solution [20]. After staining for 1 h, the sections were dried in a desiccator and examined on a JEOL JEM-100CX II transmission electron microscope (TEM) which was operated at an accelerating voltage of 80 kV.

2.4. Irradiation of electron beam

The compression-molded samples were trimmed on a Reichert–Jung Ultracut R microtome below −80°C. To avoid charging during electron irradiation a 40 nm thick gold layer was coated on the trimmed surface. The flat surfaces of the samples were irradiated with an electron beam at an accelerating voltage of 15 kV on a Philips XL 30 scanning electron microscope (SEM). The electron beam was scanned over an area of $100 \times 100\ \mu m^2$ with a line density of 484 lines/frame at a speed of 1.87 ms/line. To control the radiation dose, the beam current was calibrated with a Faraday cup. The beam current was monitored during irradiation and the beam size or filament current was adjusted slightly to keep the current in the range of 1.02–1.08 nA. This was equivalent to a dose rate of 0.102–0.108 $Cm^{-2}s^{-1}$.

2.5. Measurement of chlorine loss

The chlorine element in the irradiated layer was measured with an energy-dispersive X-ray (EDX) analyzer. The X-ray emission upon electron bombardment was detected with a lithium–silicon detector at an emission angle of 35°. The working distance was kept at 10 mm and this arrangement could give a photon count of around 6000 s^{-1}. Before starting the measurement, the instrument settings were adjusted and optimized in one region, and then the specimen was quickly moved to an adjacent position to start the measurement. This area was continuously exposed to the electron beam until the experiment was finished. An EDX spectrum consisted of the photon counts accumulated upon 110 frames of electron beam irradiation. The background was subtracted automatically by the software. The ratio of the neat intensity of the Cl K line at 2.62 keV to that of the Au M line at 2.12 keV was used to determine the amount of chlorine in the sample. It was believed that taking the Au M line as reference could minimize the effect of the fluctuation of the beam current.

3. Results and discussion

3.1. The morphological structure of PVC/NBR blends

After the sample being stained with ruthenium tetroxide, the rubber phases in the PVC/NBR blends could be identified as dark areas in the TEM view because their double bonds had combined with ruthenium tetroxide and endowed them a higher scattering capacity to electrons. Figs. 1–4 show the observed morphology of the samples blended with 10 parts of NBR-21, NBR-33, NBR-41, and NBR-51, respectively. The TEM micrograph of the PVC/NBR-21 (90/10, weight ratio) blend shows that the rubber is dispersed as irregular particles (Fig. 1) and the dimension of the rubber phase is around 0.5 μm. The boundaries between the PVC and NBR phases are rather blurred. Besides the dark rubber phase, there are many gray particles scattered in the white matrix. The grayscale of the particles is similar to that of the boundary of the rubber phase.

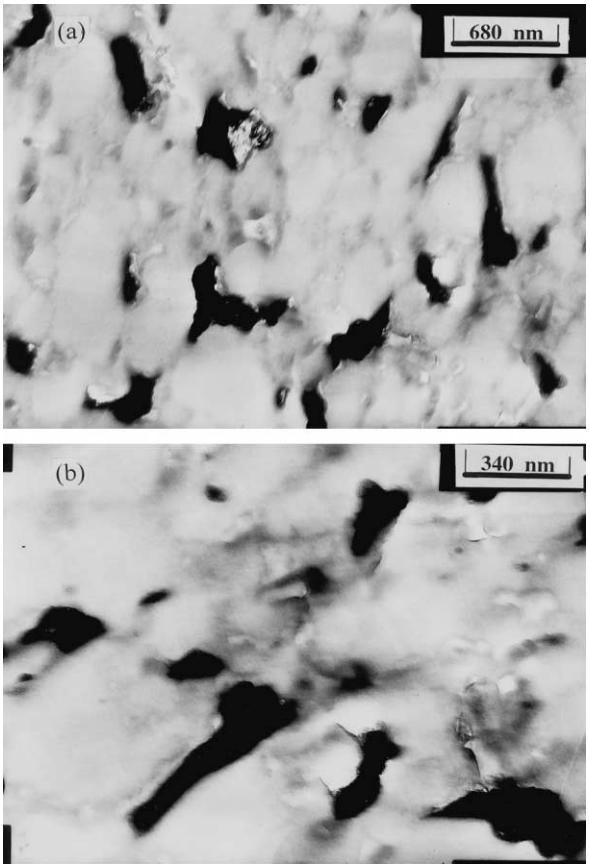

Fig. 1. Morphology of the PVC/NBR-21 (90/10) blend in the TEM view; the dark areas are rubber stained with ruthenium tetroxide.

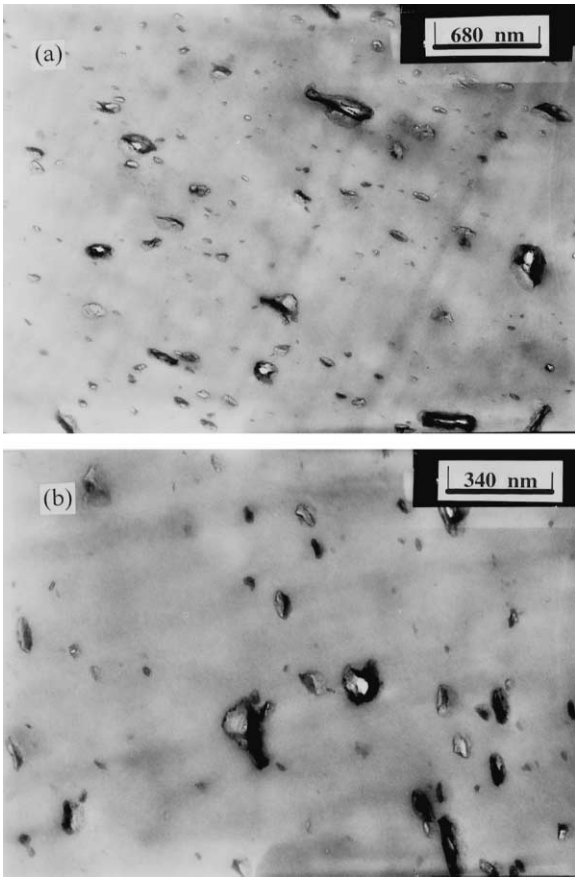

Fig. 2. Morphology of the PVC/NBR-33 (90/10) blend in the TEM view; the dark areas are rubber stained with ruthenium tetroxide.

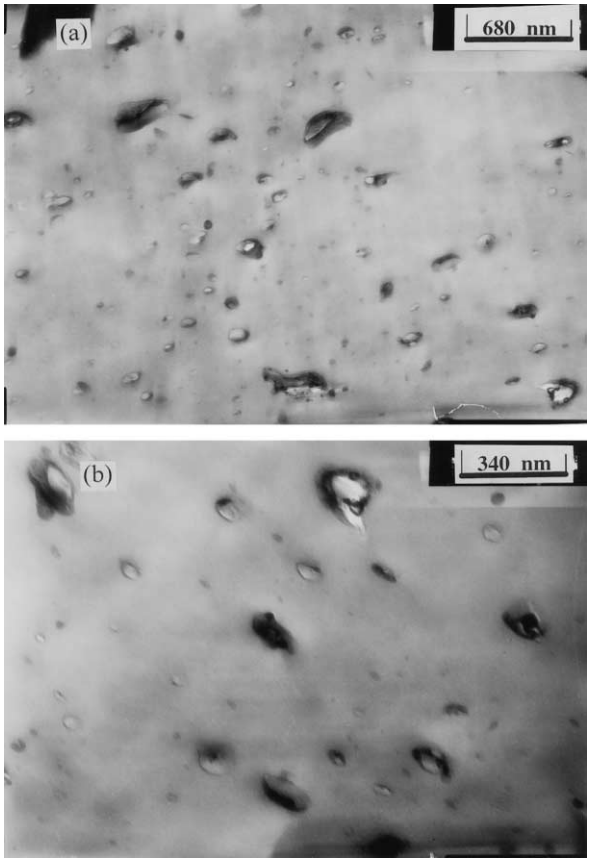

Fig. 3. Morphology of the PVC/NBR-41 (90/10) blend in the TEM view; the dark areas are rubber stained with ruthenium tetroxide.

Normally, the acrylonitrile–butadiene copolymer with approximate 20 wt% of acrylonitrile is semi-compatible with PVC because the resultant blend exhibits two glass transition temperatures and the glass transition temperature of the PVC is somewhat shifted towards low temperature [21,22]. Under moderate processing conditions the copolymer formed a continuous rubber network embedding the PVC particles and the impact strength of PVC was enhanced greatly [23]. If the blends are mixed for a longer processing time at a higher temperature or in a higher shear field, phase inversion will occur — rubber network will change into dispersed particles and PVC become the matrix [24]. The gray particles, as shown in Fig. 1, are believed to be domains of the partially mixed PVC and NBR.

It should be pointed out that some of the dark particles in the TEM micrographs are the aggregates of additives because this kind of small dark particles could be found in the section of pure PVC, as shown in Fig. 5. In this TEM micrograph, the boundary of the particles is much sharper. Also, if the cutting plan passes by near the verge of the rubber phase instead of across the middle of the rubber, the rubber phase would appear as small dark particles on the stained sections in the TEM view.

Fig. 2 shows the TEM micrograph of the PVC/NBR-33 (90/10) blend. NBR-33 is dispersed as much finer particles. The dimension of the fine particles ranges from several nm to 100 nm. Compared to the TEM micrograph of the sample of the PVC/NBR-21 blend, the intensity of the black color of the discrete phase decreases while the intensity of the gray color of the matrix increases. Furthermore, it is noted in Fig. 2 that the intensity of the black color even varies among the dispersed particles. The decrease in the intensity of the black color of the discrete phase does not come from the decrease in the concentration of the unsaturated double bonds of the copolymer because the intensity of the black color of the dispersed phase of the PVC/NBR-51 blend becomes higher (cf. Fig. 4). The change in the intensity of the black color is attributed to the change in the NBR concentration, which has resulted from the difference in compatibility, because the size of the dispersed NBR phase changes with the acrylonitrile content. Another reason is that the NBRs are not homogeneous owing to the diversity in the distribution of acrylonitrile groups in the molecules [21]. The discrete dark particles in the sample of the PVC/NBR-33 blend should not be of the pure rubber phase but of the rubber domains containing various amounts of PVC.

The morphology of the PVC/NBR-41 (90/10) blend (cf. Fig. 3) is similar to that of the PVC/NBR-33 blend except for the size distribution of the rubber-rich domains.

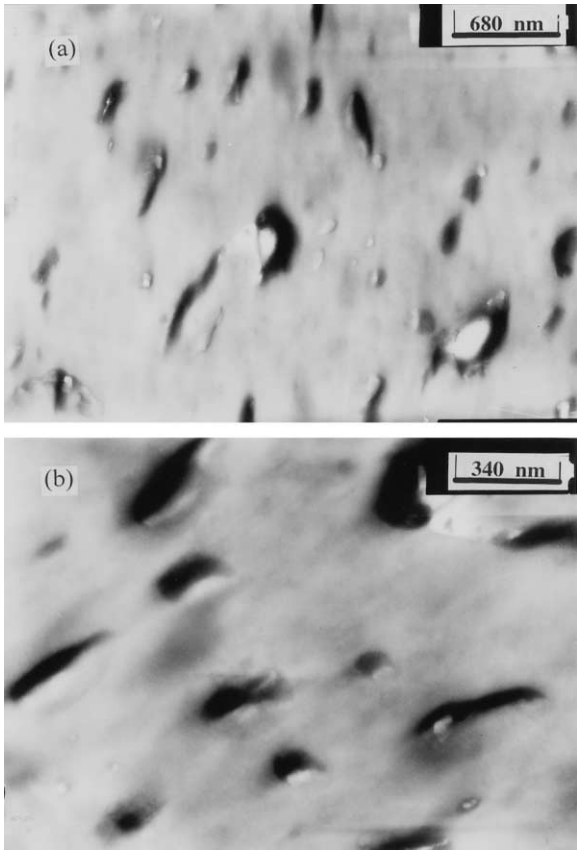

Fig. 4. Morphology of the PVC/NBR-51 (90/10) blend in TEM view; the dark areas are rubber stained with ruthenium tetroxide.

Compared to the sample of the PVC/NBR-33 blend, there are more large discrete particles, although the domain size still ranges from several nm to 100 nm. The above results indicate that the compatibility of NBR-33 is superior to that of NBR-41 because the average size of the rubber-rich domains in the PVC/NBR-33 blend is smaller than that in the PVC/NBR-41 blend.

Fig. 4 shows the observed morphology of the sample of the PVC/NBR-51 (90/10) blend. In this sample, the size of the NBR dispersed particles is larger than that of the PVC/NBR-33 and PVC/NBR-41 blends, but smaller than that of the PVC/NBR-21 blend. The size of the discrete phase ranges from 50 to 400 nm. The contrast between the discrete and continuous phases becomes higher, but not as high as that of the sample of the PVC/NBR-21 blend. In addition, the intensity of the gray color of the continuous phase is higher than that of the sample of the PVC/NBR-21 blend. Evidently, as the acrylonitrile content increases, not only the interaction between the NBR and PVC molecules but also that between NBR molecules themselves increase. It is possible that at the acrylonitrile level of 51 wt%, the attraction among NBR molecules is so strong that it suppresses the interaction between the NBR and PVC molecules. As a result, the compatibility of NBR-51 to PVC is lower than NBR-33 and NBR-41, but is higher than NBR-21. The TEM results indicate that the size of the dispersed phase is in the following order; NBR-31 < NBR41 < NBR51 < NBR21.

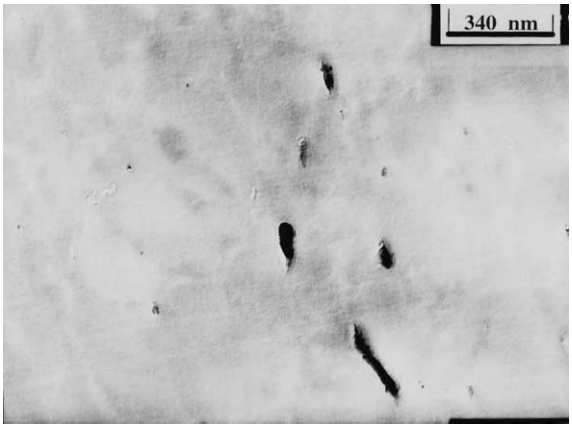

Fig. 5. Morphology of the PVC sample after ruthenium tetroxide treatment. The dark areas represent the aggregated additives.

3.2. Radiation sensitivity of PVC/NBR blends

PVC is very sensitive to electron irradiation. Under electron beam bombardment, it loses Cl continually. In the present work, the EDX spectra of different PVC/NBR blends were collected at a fixed interval of irradiation time and the decay of the intensity of Cl K line was utilized to investigate the effect of the size of the dispersed NBR in NBR/PVC blends on the radiation stability of PVC. The normalized intensity of the Cl K line against radiation dose for the samples containing 10 and 25 parts of NBR is shown in Fig. 6a and b, respectively. In these plots, the legend symbols represent the recorded experimental data and the solid lines are the best fitted curves for the experimental data. As expected the chlorine decay is very fast for pure PVC. Table 2 summarizes the doses required for the normalized intensity reaching the value of 0.7. It is obvious that the blends containing NBR, especially NBR-33 and NBR-4, have improved radiation stability of PVC. To show the radiation stability of the blends at a higher dose, Table 3 summaries the values of the normalized intensity at the dosage of 755 C m^{-2}. The normalized intensities at the exposure of 755 C m^{-2} for all the blend samples vary from 0.36 to 0.59 while that for pure PVC is 0.19. These results

Table 2
Dosage required for the normalized intensity of Cl K line reaching the value of 0.7

Sample	Dosage (C/m^{-2})		
	PVC	PVC/NBR (90/10)	PVC/NBR (75/25)
PVC	25		
PVC/NBR-21		28	35
PVC/NBR-33		90	95
PVC-NBR-41		88	52
PVC/NBR-51		32	30

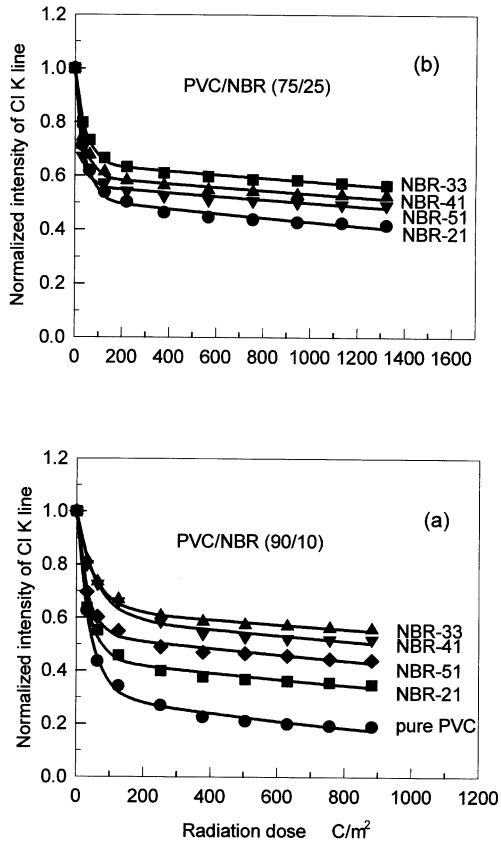

Fig. 6. Chlorine decay curves of the PVC/NBR blends upon electron beam irradiation; (a) PVC/NBR (90/10) and (b): PVC/NBR (75/25); legend symbols represent the experimental data and solid lines are the best fits of the experimental data.

further confirm that the blends are more radiation stable than pure PVC.

Fig. 6a shows that all the chlorine intensity for the blend samples containing 10 parts of NBR decreases more slowly as compared with that for the pure PVC. More importantly, the extent of the improvement is strongly related to the acrylonitrile content of the NBR. For the PVC/NBR-21 blend, only a little improvement in the radiation stability is achieved, as shown in Tables 2 and 3. As the acrylonitrile content increases to 33 wt% (NBR-33), the radiation stability of PVC is significantly enhanced. However, a further increase of the acrylonitrile content to 41 wt% (NBR-41) lead to a minor deterioration, instead of any improvement in the radiation stability of PVC. The radiation stability for the blend with NBR-51 becomes even worse but still better than that of the blend with NBR-21. The above results indicate that the protective effect of NBR on PVC against electron irradiation increases as the size of the dispersed NBR phase decreases. These results further suggest that for polymer blends containing a radiation-sensitive component, such as fluoropolymer and chloropolymer, and a radiation-insensitive component, the loss of fluorine or chlorine as a function of radiation dose can be used to investigate the size of the dispersed phase.

Table 3
The normalized intensity of Cl K line at 755 C m^{-2} exposure in different PVC/NBR blends

	NBR-21	NBR-33	NBR-41	NBR-51
PVC/NBR (90/10)	0.356	0.562	0.520	0.445
PVC/NBR (75/25)	0.438	0.587	0.541	0.507

For the blends containing 25 parts of NBR (Fig. 6b), thechlorine decay curves are similar to those blends containing 10 parts of the corresponding NBR. The protective effect for the different NBRs is in the same sequence: NBR-33 > NBR-41 > NBR-51 > NBR-21, though the radiation stability is further enhanced after addition of more NBR to PVC. The results in Table 3 show that at the same exposure all the samples with 25 parts of NBR have a higher normalized intensity than the one containing 10 parts of the corresponding NBR.

A mathematical analysis indicates that the experimental data could be fitted by a double-exponential function as shown by Eq. (3) [10,14–15]. Table 4 summarizes the best fits of the experimental chlorine-loss data for the different samples. For PVC without NBR, the calculated A value is about 0.3, while k_1 and k_2 are 2.44×10^{-2} and 6.64×10^{-4} m^2 C^{-1}, respectively. The calculated constants indicate that the dehydrochlorination rate of the fast process is almost two orders of magnitude higher than that of the slow one, and almost 70% of the Cl is lost in the fast process. After the addition of NBR, an increase in the value of A and a decrease in the value of k_2 are observed. Moreover, the value of A attains its maximum and k_2 reaches the minimum for the blends containing NBR-33. For the sample containing 25 parts of NBR-33, A is 0.64. This implies that only about 36% of the Cl is lost in the fast dehydrochlorination process after 25 parts of NBR-33 is added.

The increase in A reflects an increase in the less sensitive portion of the PVC in the blends. Though the increase in A could result from other factors, the transformation of reactive radicals to the NBR chains should play an important role. Normally, it is believed that dehydrochlorination of PVC caused by high-energy radiation undergoes a process similar to that of thermally induced dehydrochlorination [10]. An induced chlorine free radical attracts the hydrogen

Table 4
Constants obtained from the best fits of the experimental chlorine-loss data for different PVC/NBR blends

		PVC	NBR-21	NBR-33	NBR-41	NBR-51
			PVC/NBR blend (90/10)			
A		0.31	0.44	0.63	0.60	0.54
$k_1 \times 10^2$	m^2 C^{-1}	2.44	2.85	1.90	1.71	3.06
$k_2 \times 10^4$	m^2 C^{-1}	6.64	3.12	1.52	2.01	2.50
			PVC/NBR blend (75/25)			
A			0.51	0.64	0.60	0.56
$k_1 \times 10^2$	m^2 C^{-1}		2.47	2.27	2.77	3.93
$k_2 \times 10^4$	m^2 C^{-1}		1.76	1.05	1.11	1.20

of the adjacent methylene, resulting in the formation of a double bond in the PVC chain. As the allylic chlorine is active and the carbon–chlorine bond next to the double bond becomes easier to be cleaved. This will generate a chlorine radical again, resulting in a chain reaction. Thus, the dehydrochlorination can continue till an abnormal structure is met (just like a zipping reaction), leaving a conjugated polyene sequence in the PVC backbone [26]. However, after the addition of NBR to PVC, the reactive radicals, such as the chlorine radicals, can react with the unsaturated double bonds of the NBR. Another possible way to transfer the reactive radicals to the NBR molecules is that the radicals can attract the methylene hydrogen of the butadiene blocks, giving off hydrochloride and forming the less active allylic radicals in the NBR chains. All these reactions can lead to the termination of the rapid dehydrochlorination chain reaction in the PVC chains. As a result, the probability of autocatalytic dehydrochlorination is reduced, which is equivalent to a decrease in the length of the regular sequence in the PVC molecules and the increase in the concentration of the less sensitive portion. Because the chain transfer requires intimate contact between the PVC and NBR molecules, therefore, the decrease in the size of the dispersed NBR phase in the PVC/NBR blend increases the contact area between the two polymers. Thus, the decrease in the size of the dispersed NBR phase increases the less sensitive portion, i.e. the protected portion.

Kwak [19,25] demonstrated with CP/MAS ^{13}C NMR that in the PVC/NBR-30 blends there were unmixed PVC domains in a scale of a few nm. This means that not all chain segments of the PVC are mixed completely with the NBR in the blend. The dehydrochlorination of the unmixed PVC is unlikely to be strongly affected by the added NBR because there is no contact between the PVC and NBR. Hence, the constant k_1 is less affected by the addition of NBR and the value of A never approaches one. This also explains why the difference in A is small between the samples containing 10 parts and those containing 25 parts of NBR-33, while the difference is large between samples containing 10 parts and those containing 25 parts of NBR-21 or NBR-51.

4. Conclusions

The blends of PVC and NBR are heterogeneous. However, NBR-33 disperses the best in PVC and shows the highest miscibility with PVC among all the NBRs considered. The radiation stability of PVC can be improved by the addition of NBR and the extent of improvement strongly depends on the miscibility of NBR with PVC. The chlorine decay curves of the PVC/NBR blends upon electron irradiation can be fitted to Vesely's double-exponential function. The addition of NBR increases A and reduces k_2. NBR-33 provides most efficient protection to PVC and only about 37% of all PVC are highly sensitive to electron radiation at a rubber level of 10 parts. For polymer blends containing a polymer component that is radiation insensitive and another component, such as a fluoropolymer and chloropolymer that is unstable under irradiation, the loss of fluorine or chlorine as a function of radiation dose can be used to determine the size of the dispersed phase of polymer blends.

Acknowledgements

This work was supported by the Hong Kong Government Research Grant Council under the grant No. HKUST 6033/98P.

References

[1] Ivanov VS. Radiation chemistry of polymers. Utrecht, The Netherlands: VSP, 1992.
[2] Grassie N, Scott G. Polymer degradation stabilisation. Cambridge: Cambridge University Press, 1988.
[3] Singh A, Silverman J. Radiation processing of polymer. New York: Hanser Publishers, 1992.
[4] Clegg D, Collyer AA. Irradiation effect on polymers. London: Elsevier, 1991.
[5] Miller AA. In: Dode M, editor. The radiation chemistry of macromolecules, vol. II. 1973 (Chapter 10).
[6] Azuma C, Sanui K, Ogata N. J Appl Polym Sci 1980;25:1273.
[7] Schultz AR, Mankin GI. J Polym Sci Polym Symp 1976;54:341.
[8] Nguyen TQ, Kausch HH. J Appl Polym Sci 1984;29:455.
[9] Lindberg KA, Vesely D, Bertilsson HE. J Mater Sci 1989;24:2825.
[10] Vesely D, Finch DS. Ultramicroscopy 1987;13:329.
[11] Delgado LA, Hutchinson TE. Ultramicroscopy 1979;4:163.
[12] Isaacson MS. In: Hayat M, editor. Principles and techniques of electron microscopy. New York: Van Nostrand-Reinhold, 1977.
[13] Egerton RF. Ultramicroscopy 1980;5:521.
[14] Vesely D. Ultramicroscopy 1984;14:279.
[15] Lindberg KA, Vesely D, Bertilsson HE. J Mater Sci 1985;20:2225.
[16] Zhu SH, Chan CM. Macromolecules 1998;31:1690.
[17] Zakrzewski GA. Polymer 1973;14:347.
[18] Sen AK, Mukherjee GS. Polymer 1993;34:2386.
[19] Kwak SY, Nakajima N. Macromolecules 1996;29:5446.
[20] Li JX, Ness JN, Cheung WL. J Appl Polym Sci 1996;59:1733.
[21] Terselius B, Ranby B. Pure Appl Chem 1981;53:421.
[22] Matsuo M, Nozaki C, Jyo Y. Polym Engng Sci 1969;13:1585.
[23] Zhu ZH, Chan CM. Polymer 1998;39:7023.
[24] Landi VR. Appl Polym Symp 1974;25:223.
[25] Kwak SY, Nakajima N. Polymer 1996;37:195.
[26] Yassin AA, Sabaa MW. J Macromol Sci — Rev Macromol Chem Phys 1990;C30:491.